

PAPER • OPEN ACCESS

Structural and magnetic analysis of the $\text{Pr}_{1.5}\text{Eu}_{1.5}\text{Ba}_5\text{Cu}_8\text{O}_{18}$ system

To cite this article: J A Parra-Borda *et al* 2017 *J. Phys.: Conf. Ser.* **935** 012005

View the [article online](#) for updates and enhancements.

Related content

- [Magnetic Analysis of Plasma Configuration in Tokamak Experiment Using Boundary Element Method](#)
Kazuhiro Takeuchi, Mitsushi Abe, Hideshi Fukumoto *et al.*
- [Increasing the efficiency of the condensing boiler](#)
O N Zaytsev and E A Lapina
- [Increasing the efficiency of the condensing boiler](#)
ON Zaytsev and EA Lapina

Structural and magnetic analysis of the $\text{Pr}_{1.5}\text{Eu}_{1.5}\text{Ba}_5\text{Cu}_8\text{O}_{18}$ system

J A Parra-Borda¹, F G Rojas-Cruz¹, A F Cruz-Pacheco², S Segura-Peña^{1,2} and C A Parra Vargas²

¹ Universidad Santo Tomás, Tunja, Colombia

² Universidad Pedagógica y Tecnológica de Colombia, Tunja, Colombia

E-mail: sully.segura01@usantoto.edu.co

Abstract. This research describes the synthesis and characterization of the $\text{Pr}_{1.5}\text{Eu}_{1.5}\text{Ba}_5\text{Cu}_8\text{O}_{18}$ system, obtained by the solid-state reaction method. For the synthesis of this material, oxides of Pr_6O_{11} , Eu_2O_3 , BaO and CuO were used. The sintering temperature was 900°C . The structural analysis of the synthesized systems was carried out using X-Ray Diffraction (XRD), with a comparison with theoretical patterns and validated with Rietveld refinement analysis, obtaining a type $P2mm$ crystallographic orthorhombic system with $a=3.892454\text{\AA}$, $b=3.894411\text{\AA}$ and $c=31.155851\text{\AA}$. The characterization by means of Scanning Electron Microscopy (SEM) let us conclude that the material presents homogeneous granular morphology. Finally, the magnetic response of this material is determined by the magnetization curves as a function of the applied magnetic field 50K and as a function of temperature 2000Oe.

1. Introduction

Crystallographically, the perovskite type materials are represented by the general expression ABO_3 , where A is a representative element and B is a transition metal which has a smaller ionic radius than the cation at position A [1-3]. In recent years attention has been paid to the incorporation of earth elements into the position of cation A, since these atoms create structural defects that allow the achievement of certain characteristics and properties, in particular ferromagnetic and superconducting ones, the most of the rare earths in their valence state $3+$. And in coordination site VIII they have a similar radius and therefore can be replaced in different systems forming the same crystalline structure.

Currently, much interest has arisen about oxide composites with perovskite type materials due to their diversity of crystalline structures and physical properties; these compounds are known for having unique properties such as ferroelectricity, electrical conductivity, superconductivity and magnetoresistance that can be used in different technological and industrial applications [4]. Some of the most relevant applications of this type of materials are the superconducting magnets [5], electric motors [6] and magnetic shields [7].

One of the most important perovskite type materials for superconductive applications are compounds such as $\text{YBa}_2\text{Cu}_3\text{O}_7$, Bi-2223 and $\text{REBa}_2\text{Cu}_3\text{O}_7$, where RE refers to a rare earth element such as Nb, Nd, Sm, Gd, Eu, among others. The most used material for research in terms of superconducting properties is $\text{YBa}_2\text{Cu}_3\text{O}_7$ since this one presents a great facility in its synthesis process and it has excellent superconducting properties [8] due to its characteristics, thus, allowing the



modelling of complex systems to explain their electrical and magnetic properties. The development of these models has contributed to the creation of more complex systems, among them Re124, Re358 [9], which have ostensibly improved its characteristics. Many compounds with different stoichiometric weights have been used structurally varying the primitive cell of the perovskite, which can present a simple, or rather complex structure depending on the amount of rare earth atoms that are arranged in its stoichiometry. It is necessary to highlight that one of the first compounds is from the Y123 family [10].

The properties of these compounds and its use in various technologies are affected by the synthesis method applied, in which, parameters such as purity of the precursors and temperature, are indispensable for the improvement of the magnetic and morphological structural properties. For this reason, this work pretends to enhance the above described characteristics for the Re358 type compound through the new $\text{Pr}_{1.5}\text{Eu}_{1.5}\text{Ba}_5\text{Cu}_8\text{O}_{18}$ system, synthesized by means of the solid state reaction method, using high purity precursor oxides.

2. Experimental

The $\text{Pr}_{1.5}\text{Eu}_{1.5}\text{Ba}_5\text{Cu}_8\text{O}_{18}$ system was synthesized by using the standard method of solid-state reaction (SSR) [11]. Stoichiometric amounts of Pr_6O_{11} (99.9%), Eu_2O_3 (99.9%), BaO (99.99%) and CuO (99.999%) oxides were used. The oxides were mixed and macerated for 4 hours, it was compressed at a pressure of 5MPa and were calcined at a temperature of 850°C for 34 hours. The synthesis process was made at 900°C for 34 hours. After completing the previously described stages of the process, the synthesized and oxygenated correspondent final stage was carried out. The sample was set at a synthesis temperature of 900°C, with a ramp for this process that lasted a 116-hour period, and when 44 hours had passed, the oxygenation process started, and coming to an end when it arrived at a temperature of 450°C. The sample oxygenated process lasted approximately 51.5 hours. An oxygen flux of 100mL/min followed by slow cooling at 300°C was used and lasted 9 hours until achieving room temperature.

The structural characterization of the sample was analysed by XRD Method, in a PAN'alitics PRO "MPD" diffractor, equipped with an accelerator detector X 'Ultra-Fast' and Bragg-Brentano configuration, using $\text{Cu K}\alpha$ ($\lambda=1.54186\text{\AA}$) between 20° y 90°. The measurements were performed with a tension of 40kV and a current of 20mA [2]. For the Rietveld refinement analysis PCW and GSAS software was used. The refinement was made with the purpose of establishing the network parameters that make up this new material.

3. Results and discussion

3.1. Structural analysis

For the elaboration of a theoretical Rietveld plot and the refinement of the system $\text{Pr}_{1.5}\text{Eu}_{1.5}\text{Ba}_5\text{Cu}_8\text{O}_{18}$ the superconducting material Y358 [12] was taken as a reference point. Figure 1 shows the analysis of Rietveld refinement, where you obtained a cell with a crystallographic space group P2mm and the following parameters: $a=3.892454\text{\AA}$, $b=3.894411\text{\AA}$ and $c=31.155851\text{\AA}$; this structure has been reported as perovskite-orthorhombic [13]. Figure 2 shows the structure of the system, and the crystallographic cell in the Table 1 shows the refined atomic positions and occupations of the Pr358. A comparison between theoretical Rietveld plot and the experiment shows evidence of the emergence of two impurities, $\text{PrBa}_2\text{Cu}_3\text{O}_7$ and BaO which can be removed if the sintering temperature is increased. With the refinement we found a $\chi^2=4.6$ and $R(F^2)=0.09\%$ 0.0742 error.

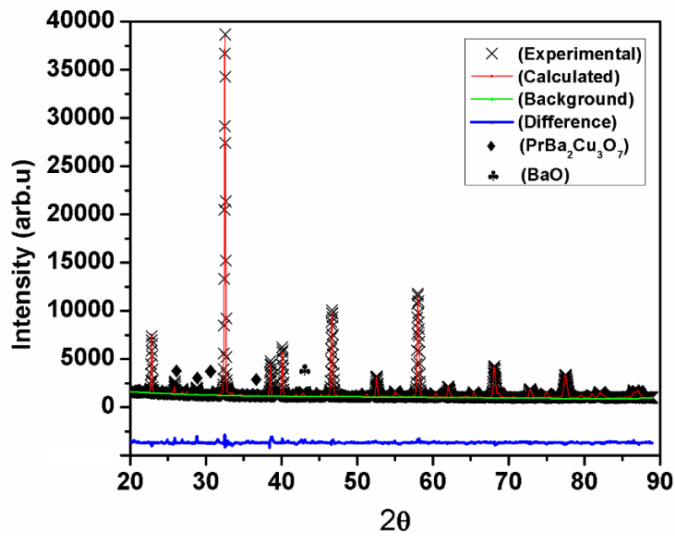


Figure 1. Rietveld refining of the sample $\text{Pr}_{1.5}\text{Eu}_{1.5}\text{Ba}_5\text{Cu}_8\text{O}_{18}$ through the general structure analysis of the program (GSAS).

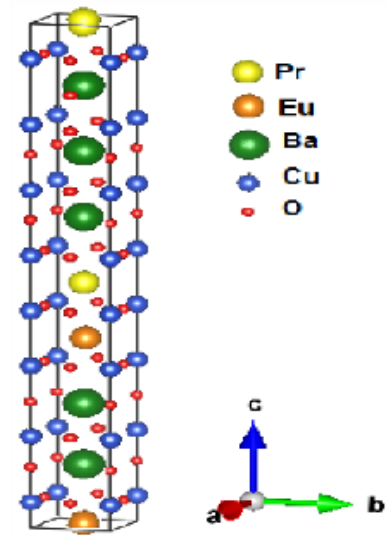


Figure 2. Crystal structure of $\text{Pr}_{1.5}\text{Eu}_{1.5}\text{Ba}_5\text{Cu}_8\text{O}_{18}$ obtained with the Vesta software.

Table 1. Refining of the atomic positions and atoms occupancy in the sample $\text{Pr}_{1.5}\text{Eu}_{1.5}\text{Ba}_5\text{Cu}_8\text{O}_{18}$.

Atoms	x	Y	z	Occupancy
Pr(1)	0.5263	0.6552	0.0000	0.3871
Eu(1)	0.4968	1.5716	0.0000	0.4141
Pr(2)	0.5465	0.6093	0.3547	0.5307
Eu(2)	0.4163	1.4368	0.3628	0.4561
Pr(3)	0.4174	0.5000	0.5156	0.4775
Eu(3)	0.5381	0.5000	0.5117	0.5861
Pr(4)	0.5706	0.5000	0.0334	0.4862
Eu(4)	0.3783	0.5000	0.0128	0.4854
Ba(1)	0.4754	0.5256	0.1191	0.9553
Ba(2)	0.5371	0.3520	0.2212	0.9021
Ba(3)	0.5032	0.5000	0.3871	0.9923
Ba(4)	0.4777	-0.4677	0.2512	0.8563
Ba(5)	0.5144	0.5000	0.8571	0.8672
Cu(1)	1.0256	0.0000	0.9420	1.0000
Cu(2)	1.0019	0.0000	0.8129	0.8507
Cu(3)	1.0239	0.0000	0.6865	1.0000
Cu(4)	0.9892	0.0000	0.5627	0.9655
Cu(5)	0.9965	0.0000	0.4379	0.9685
Cu(6)	1.0248	0.0000	0.3176	1.0000
Cu(7)	1.0021	0.0000	0.1940	0.8626
Cu(8)	1.0073	0.0000	0.0690	1.0000
O(1)	0.4388	0.0000	0.9466	0.9202

O(2)	1.0320	0.5000	0.9747	1.0000
O(3)	1.0624	0.0000	0.8999	1.0000
O(4)	0.0472	0.1267	0.8204	1.0000
O(5)	1.0820	0.0000	0.7706	1.0000
O(6)	0.5333	0.0000	0.6974	1.0000
O(7)	1.0843	0.5000	0.6829	0.4031
O(8)	0.5220	0.0000	0.5648	0.9203
O(9)	1.0050	0.5000	0.5747	0.9971
O(10)	0.5677	0.0000	0.4261	0.6453
O(11)	0.0221	0.4459	0.4407	1.0000
O(12)	1.0104	0.0000	0.3557	1.0000
O(13)	0.0367	0.6075	0.3167	1.0000
O(14)	1.0535	0.0000	0.2328	0.7458
O(15)	-0.0460	1.1201	0.2095	1.0000
O(16)	0.0095	-3.4793	0.1777	1.0000
O(17)	0.4384	0.0000	0.0533	0.9088
O(18)	1.0430	0.5000	0.0382	0.9699

3.2. Morphological analysis

Figure 3 shows the results obtained through SEM for different magnifications \times (3000, 5000 and 10000) of a cross-section taken for the sample $\text{Pr}_{1.5}\text{Eu}_{1.5}\text{Ba}_5\text{Cu}_8\text{O}_{18}$, in which there is a clear presence of porosity, and the grain size is not uniform, indicating that the sintering process which was carried out for this sample is not satisfactory [14].

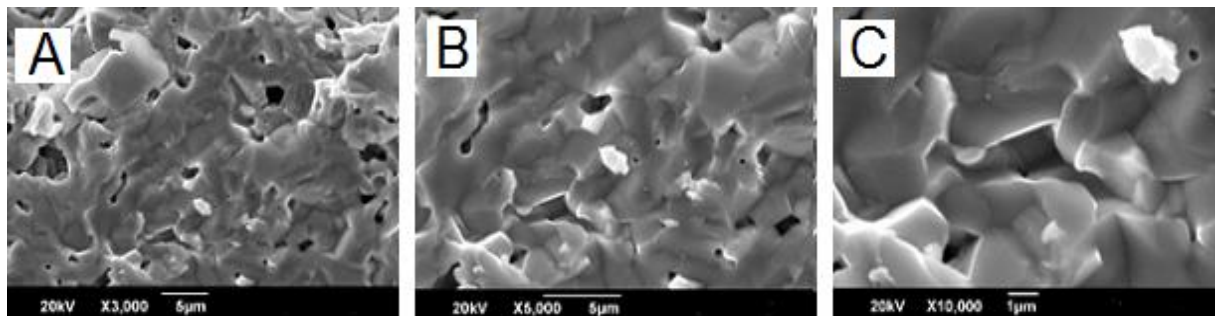


Figure 3. SEM images for the cross section of $\text{Pr}_{1.5}\text{Eu}_{1.5}\text{Ba}_5\text{Cu}_8\text{O}_{18}$ with different magnifications, increases (A) 3000, (B) 5000, (C) 10000.

Figure 4 shows the results obtained through SEM for three magnifications \times (3000, 5000 and 10000) that correspond to the superficial part of the material. It is evident the presence of porosity in different parts of the material, and coplanar defects at high and low angles but presents domain in the crystallographic size between 10 and 20nm, which is in agreement with the results obtained by XRD. As reported in the references [12] and [15], the grain size of the sample is a function of the oxygen content applied to it, therefore, the samples of $\text{Pr}_{1.5}\text{Eu}_{1.5}\text{Ba}_5\text{Cu}_8\text{O}_{18}$ must have a process of oxygenation.

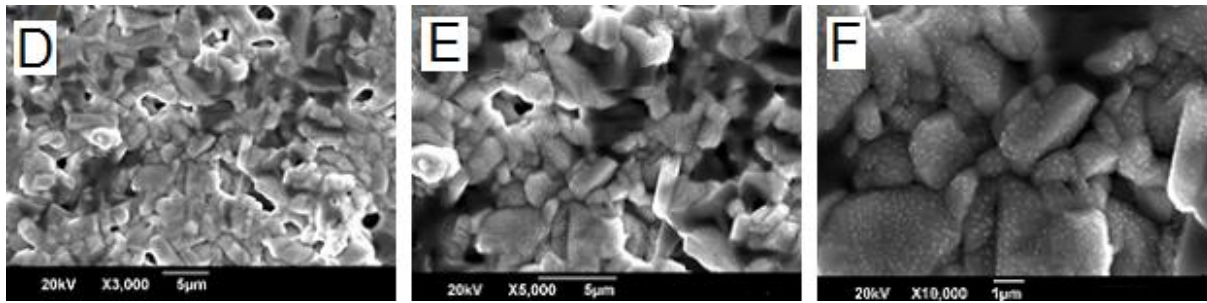


Figure 4. Images of SEM, surface part of samples $\text{Pr}_{1.5}\text{Eu}_{1.5}\text{Ba}_5\text{Cu}_8\text{O}_{18}$ at different magnifications, increases (D) 3000, (E) 5000, (F) 10000.

3.3. Magnetic properties

This test was carried out in a commercial magnetometer, with a SQUID (Superconducting Quantum Interference Device) sensor, Quantum Design (MPMS-5S) device. Figure 5 shows the graph of magnetization as a function of the magnetic field at a constant temperature of 50K. The curve shows the typical behaviour of a paramagnetic material, as that can be seen in Figure 6, a graphic of magnetic susceptibility as a function of the temperature, at a constant magnetic field of 200Oe, which follows the law of Curie. At the same time at right top of the graph, the inverse of the magnetic susceptibility was plotted as a function of temperature. The slope of the graph determines the effective magnetic moment of the sample, from which it was obtained a value for $\text{Pr}_{1.5}\text{Eu}_{1.5}\text{Ba}_5\text{Cu}_8\text{O}_{18}$ of $5.74\mu_B$ and a theoretical effective magnetic moment of $5.79\mu_B$ [16].

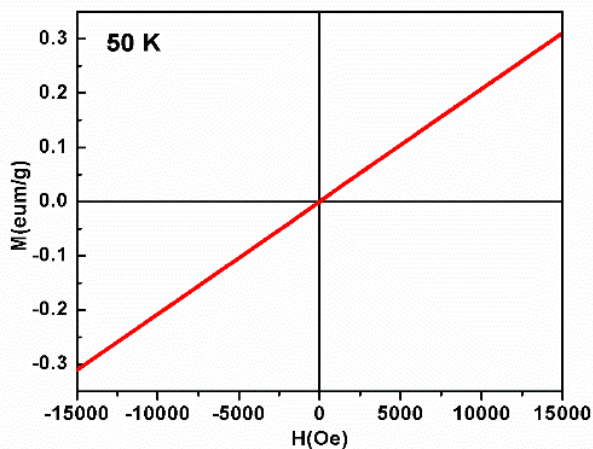


Figure 5. M vs H curves of $\text{Pr}_{1.5}\text{Eu}_{1.5}\text{Ba}_5\text{Cu}_8\text{O}_{18}$ samples at 50 K.

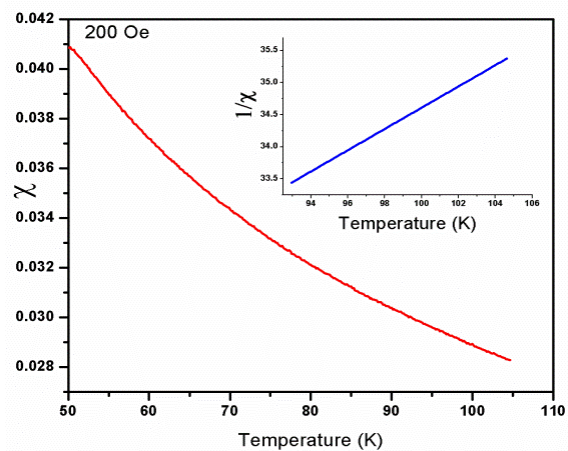


Figure 6. Susceptibility curve and its inverse susceptibility curve for sample $\text{Pr}_{1.5}\text{Eu}_{1.5}\text{Ba}_5\text{Cu}_8\text{O}_{18}$.

4. Conclusion

Using the method of solid-state reaction for the sintering of the new material $\text{Pr}_{1.5}\text{Eu}_{1.5}\text{Ba}_5\text{Cu}_8\text{O}_{18}$ with orthorhombic perovskite type structure and space group 25 with network parameters $a=3.8960\text{\AA}$, $b=3.8890\text{\AA}$ and $c=31.1500\text{\AA}$. The structural characterization of the sample was made with X-ray diffraction finding the main phase to be Pr358. It also showed the evidence of secondary phases. The secondary phase, which manifested itself in a greater proportion, was $\text{PrBa}_2\text{Cu}_3\text{O}_7$. The effective magnetic moment of the samples was obtained and it is expected the thermal and oxygenated processes to be performed in a slower way, in order to reach the superconducting state.

References

- [1] Alvarado Flores J J 2016 Análisis de la estructura perovskita $\text{La}_x\text{Sr}_{1-x}\text{Cr}_y\text{Mn}_{1-y}\text{O}_{3-\delta}$ con potencial aplicación como ánodo para celdas de combustible de óxido sólido *Boletín la Soc. Española Cerámica y Vidr.* **56** 73–82
- [2] Abdel-Aal S K 2017 Synthesis, characterization, thermal, and electrical properties of new diammonium hybrid perovskite $[\text{NH}_3(\text{CH}_2)_7\text{NH}_3]\text{CaCl}_2\text{Br}_2$ *Solid State Ionics* **303** 29–36
- [3] Nishiyama A, Doi Y and Hinatsu Y 2017 Magnetic interactions in rhenium-containing rare earth double perovskites $\text{Sr}_2\text{LnReO}_6$ (Ln=rare earths) *J. Solid State Chem.* **248** 134–141
- [4] Fujimoto H 2003 Flexural strength of melt-processed Y–Ba–Cu–O bulk superconductors with Ag addition measured at 77 K *Supercond. Sci. Technol.* **16** 1115–1119
- [5] Jirsa M, Rameš M, Ďuran I, Melíšek T, Kováč P and Viererbl L 2017 Electric currents in REBaCuO superconducting tapes *Supercond. Sci. Technol.* **30** 45010
- [6] Kawamura M and Jones J A 2017 Superconducting Super Motor and Generator *IEEE Trans. Appl. Supercond.* **27** 1–5
- [7] Terao Y, Sekino M, Ohsaki H, Teshima H and Morita M 2011 Magnetic Shielding Characteristics of Multiple Bulk Superconductors for Higher Field Applications *IEEE Trans. Appl. Supercond.* **21** 1584–7
- [8] D.A.LandinezTellez, H.Tovar O O-D J R 2007 Estructura cristalina del nuevo oxido tipo perovskita compleja $\text{Ba}_2\text{NdZrO}_5$ *Rev. Mex. Fis.* **S53** 299–302
- [9] F P-C, J A-S and H T-H 2013 Contribución de los orbitales f en la densidad de estados de los superconductores $\text{NdBa}_2\text{Cu}_3\text{O}_7$ y $\text{SmBa}_2\text{Cu}_3\text{O}_7$ *Superf. y Vacío* **26** 84–89
- [10] Gutiérrez S S, G I S, Roa-Rojas J and Vargas C A P 2016 Production a characterization of new system superconductor $\text{TR}_3\text{Ba}_8\text{Cu}_{11}\text{O}_8$ *J. Phys. Conf. Ser.* **687** 12089
- [11] Vargas C A P, Jr. J L P, Pureur P, Téllez D A L and Roa-Rojas J 2012 Behavior of the irreversibility line in the new superconductor $\text{La}_{1.5+x}\text{Ba}_{1.5+x-y}\text{Ca}_y\text{Cu}_3\text{O}_z$ *Phys. B Condens. Matter* **407** 3128–3130
- [12] Gholipour S, Daadmehr V, Rezakhani A T, Khosroabadi H, Shahbaz Tehrani F and Hosseini Akbarnejad R 2012 Structural Phase of Y358 Superconductor Comparison with Y123 *J. Supercond. Nov. Magn.* **25** 2253–2258
- [13] Pacheco A F C, Cuaspud J A G and Vargas C A P 2017 Synthesis, characterization and magnetic evaluation of praseodymium modified cerium oxide *J. Phys. Conf. Ser.* **786** 12023
- [14] Guerrero U F, Parra Vargas C A and Santos A S 2011 Procesamiento en descarga luminiscente de la perovskita $\text{YBa}_2\text{Cu}_3\text{O}_{7-d}$ **78** 201–205
- [15] Hurtado P C P, Téllez D A L, Vásquez J A C, Vargas C A P and Roa-Rojas J 2015 Synthesis, structural characterization, electric and magnetic behaviour of a $\text{Sr}_2\text{DyNbO}_6$ double Perovskite *J. Phys. Conf. Ser.* **614** 12002
- [16] Gómez J A M, García G I S, Palacio C A and Vargas C A P 2015 Production and structural and magnetic characterization of a $\text{Bi}_{1-x}\text{Y}_x\text{FeO}_3$ ($x = 0, 0.25$ and 0.30) system *J. Phys. Conf. Ser.* **614** 12003